Bone 123 (2019) 211–223

Contents lists available at ScienceDirect

Bone

journal homepage: www.elsevier.com/locate/bone

Full Length Article

Inverse correlation between trabecular bone volume and bone marrow adipose tissue in rats treated with osteoanabolic agents

Samantha Costa, Heather Fairfield, Michaela R. Reagan*

Maine Medical Center Research Institute, Scarborough, ME, USA
University of Maine Graduate School of Biomedical Science and Engineering, Orono, ME, USA
Tufts University School of Medicine, Boston, MA, USA

ARTICLE INFO

Keywords:
Bone marrow adipose
Sclerostin
Bone marrow microenvironment
Osteocyte-derived factors
Anti-sclerostin antibodies
Parathyroid hormone
PTH

ABSTRACT

There is currently an unmet clinical need for improved treatments for skeletal diseases such as osteoporosis and cancer-induced bone disease. This is due in part to a paucity of novel targets and an incomplete understanding of the mechanisms of action for established therapies. We defined the effects of anabolic treatments on bone and the bone marrow adipocyte (BMA). Sclerostin-neutralizing antibodies (Scl-Ab), romosozumab, human parathyroid hormone (hPTH, 1–34), and hPTH/hPTHrP analogues (e.g. teriparatide and abaloparatide) stimulate bone formation and have been studied in clinical trials for severe osteoporosis. In this study, eight-week-old male and female rats were administered vehicle, Scl-Ab (3 mg/kg or 50 mg/kg) weekly, or hPTH (1–34) (75 μg/kg) daily for 4 or 26 weeks. Histological analyses of distal femura were performed using a novel ImageJ method for trabecular bone and bone marrow adipose tissue (BMAT). Adipocyte number, circumference, and total adipose area were compared within the tissue area (T.Ar) or the marrow area (Ma.Ar), (defined as the T.Ar minus the trabecular bone area). After 26 weeks of treatment, a significant inverse correlation between bone and tissue adiposity (total adipocyte area divided by T.Ar) were observed in males and females ($p < 0.0001$). However, there were no significant correlations between bone and marrow adiposity (total adipocyte area divided by Ma.Ar) for either sex after 26 weeks of treatments. Scl-Ab treatments also resulted in no effect on adipocytes based on marrow adiposity for either sex after 26 weeks. However, chronic hPTH treatments significantly reduced adipocyte number and adiposity within the T.Ar and within the Ma.Ar in males. Overall, our data suggest that with long-term treatment, Scl-Abs decrease total tissue adiposity mainly by increasing trabecular bone, resulting in an overall reduction in the space in which adipocytes can reside. These findings were determined by developing and comparing two different methods of assessment of the marrow cavity, defined to either include or exclude trabecular bone. Thus, researchers should consider which adiposity measurement is more informative and relevant for their studies. Overall, our findings should help design improved therapies or combination treatments to target a potential new contributor to bone diseases: the bone marrow adipocyte.

1. Introduction

Adequate bone mass is essential for a long, healthy life in humans and other vertebrates. Along with signaling throughout the body, coordinated signaling between bone cells through paracrine, autocrine, and endocrine pathways is critical to metabolic homeostasis of the skeleton and bone marrow (BM) microenvironment [2,3]. Skeletal stability is maintained through balanced osteoblastic and osteoclastic activity, resulting in cyclic bone resorption and formation mediated by coupling between osteoclasts and osteoblasts. However, BM adipocytes, derived from a common adipo-osteoprogenitor cell, also play a crucial role in bone homeostasis. Increased BM adiposity is often correlated with bone diseases, such as osteoporosis, diabetic bone disease, and cancer-associated osteolysis, and BM adipocytes have been shown to respond to a variety of pharmaceuticals, therapies, diets and disease conditions [2,4–9]. Interestingly, stimuli or states that increase bone mass (e.g. mechanical loading, osteoanabolic pharmaceutical treatments, and genetic diseases, such as van Buchem disease and sclerosteosis) often correlate with decreased bone marrow adipose tissue (BMAT). Similarly, diseases and models of bone loss typically display increased BMAT [1,2,4]. However, BMAT appears to be essential in the homeostasis of the hematopoietic niche after insults such as irradiation [10], although excessive BMAT can also be detrimental to hematopoiesis [11]. Thus, understanding the short-term and chronic effects of

* Corresponding author at: Center for Molecular Medicine and Center for Translational Research, 81 Research Drive, Scarborough, ME 04074, USA.
E-mail address: Mreagan@mmc.org (M.R. Reagan).

https://doi.org/10.1016/j.bone.2019.03.038
Received 16 October 2018; Received in revised form 26 March 2019; Accepted 28 March 2019
Available online 04 April 2019

increasing bone mass on BMAT will help define the elusive relationship between bone and adipose tissue, which may help clarify the roles of BMAT in disease and recovery. Moreover, understanding the effects of bone anabolic agents on BM adipocytes would give new insight into the mechanisms of action of pharmaceuticals and provide information about the osteoblast-adipocyte relationship.

Sclerostin-neutralizing antibodies (Scl-Ab) and human parathyroid hormone (hPTH) increase bone mass in rats, mice, and humans through different modes of action at the tissue level and through different signaling pathways [1,12]. In the rat model described by Ominsky et al. [1], Scl-Ab increase trabecular and cortical bone mass by binding to sclerostin, which then prevents sclerostin from binding to frizzled co-receptors lipoprotein receptor protein 4/5/6, inhibiting canonical Wnt signaling [12,13]. This neutralizing effect allows for Wnt signaling and subsequent activation and differentiation of mesenchymal stromal cells (MSCs) into osteoblasts, which increase modeling-based bone formation [2,13]. Scl-Ab also suppress bone resorption through inhibitory effects on osteoclasts via modulation of several osteoclastogenesis regulators such as M-CSF, WISP1, and the RANKL/osteoprotegerin (OPG) ratio [1,12,14–16]. Previously, Scl-Ab were shown to increase bone formation and decrease BMAT in 6-week old male mice after only 3 weeks of 100 mg/kg/week treatment [2,17]. Interestingly, in vitro studies showed that adipocyte progenitor cells increase in their Oil Red O content, increase their expression of adipogenic genes (*PPARγ* and *CEBPα*), and decrease their expression of β-catenin responsive genes (*Axin2* and *Smad6*) when treated with sclerostin, suggesting that the in vivo findings of decreased BMAT in response to Scl-Ab were at least partially due to a shifting of the differentiation of skeletal MSCs from the adipogenic to the osteogenic pathway [2]. Still, as in vivo responses may not mirror those seen in vitro, it would have been beneficial to analyze changes in progenitor cells in vivo to determine what occurred more conclusively.

In contrast to Scl-Ab, hPTH substantially increases both bone anabolic (formation) and catabolic (resorption) activities, although the former is more pronounced during the first few months of therapy in humans. hPTH stimulates osteogenesis in $PTH1R^+$ osteoprogenitors [18] and increases the activity of mature osteoblasts, resulting in increased bone formation and bone mass [1,2,19]. This activation may be in part due to enhanced Wnt signaling, but other pathways are certainly operative [18,20]. Unlike Scl-Ab, hPTH stimulates bone resorption through enhanced RANKL production in stromal cells [21]. In fact, the bone anabolic action of hPTH appears to depend on its ability to indirectly stimulate osteoclastogenesis [21]. However, hPTH also inhibits osteoblast apoptosis and reduces osteocytic production of sclerostin [21]. Thus, in both animal and human models, hPTH action is dependent upon increased bone resorption, which induces bone remodeling and formation, resulting in a net gain in bone mass (depending on dosing levels and frequency) [1]. Prior studies also found that hPTH could decrease BMAT associated with energy restriction in calorically-restricted rats, although this was done in older male, Fischer 344 rats with much lower hPTH doses (1 μg/kg/day for 14 days) [22]. In mice, Lanske et al. observed short-term hPTH treatments can decrease BMAT in mice [23]. Interestingly, Kronenberg et al. recently demonstrated that sudden cessation of teriparatide after prolonged administration in mice led to increased adipocytic differentiation of descendants of *Sox9*-creERT2 cells, leading to a massive increase in BMAT, which was not observed in controls [24]. These data suggest that hPTH increases the number of adipo-osteoprogenitor cells in the BM, and that these will become osteoblasts if they receive sustained hPTH signaling or adipocytes if the hPTH signal is removed.

To our knowledge, no studies of longer-term hPTH or Scl-Ab treatments on BMAT in rats have been previously reported. We hypothesized that Scl-Ab and hPTH treatments would decrease overall adiposity in a time-dependent and dose-dependent manner, and that a negative correlation would be identified between bone and BMAT areas. We also hypothesized that the results would depend on if we looked at adiposity within the marrow area (lacking trabecular bone) or in the larger tissue area of the ROI. Lastly, we hypothesized that there would be sex-based differences in adiposity and response to anabolic agents. To test these theories, we developed and described a new ImageJ analysis method to quantify BMAT from histological slides. We used this method to determine how BM adipocytes are affected by Scl-Ab and hPTH treatments within the marrow area and total tissue area by defining and measuring these two different areas. (The tissue area represents the larger overall bone marrow cavity that provided information on adiposity in relation to increased bone and decreased marrow space. The marrow area excluded bone accrual differences per treatment group to identify an adipocyte-specific niche where adipocyte parameters could be analyzed in response to these osteoanabolic agents). No other method allows for this dual analysis within the same histology slide, and no reports comparing these different methods of analysis have been described to our knowledge. We then explored the dependence of BMAT and bone on length of treatment, dose, and sex, and tested correlations between BMAT and bone area using a linear regression statistical model.

2. Methods

2.1. Study design and histological slide preparation

The effects of Scl-Ab (romosozumab) and hPTH (1–34) on BMAT were tested through analysis of histological slides of rat distal femurs stained with Von Kossa tetrachrome, which were generated in a previously published study [1]. In that study, 2-month old male and female Sprague-Dawley rats were obtained from the Charles River Laboratory (Hollister, CA) and divided into four treatment groups: Vehicle (n = 20/sex), Scl-Ab 3 mg/kg (n = 70/sex), Scl-Ab 50 mg/kg (n = 38/sex), or hPTH 75 μg/kg (n = 20). Scl-Ab (romosozumab, 34.97 mg/mL) or the vehicle (55 mM acetate, 13 mM calcium, 6% sucrose, 0.006% polysorbate 20, pH 5.2) were administrated once weekly via subcutaneous (SC) injection. Due to romosozumab, a humanized Scl-Ab, having immunogenic properties in rodents, Scl-Ab groups reserved the right to remove rats that developed anti-drug antibodies (ADA) since ADAs can attenuate pharmacological effectiveness. hPTH (1–34) was administered daily via SC injection. The hPTH (1–34) was reconstituted in sterile water and diluted to 0.15 mg/mL in a buffer solution (2% bovine serum albumin, 0.001 N HCl, 0.15 M NaCl) for a dosage volume of 0.5 mL/kg. One cohort of rats was dosed for a total of 4 weeks; a second cohort was dosed for 26 weeks.

The standardized criteria for structural, dynamic, and cellular parameters established by the American Society for Bone and Mineral Research were used when determining proper nomenclature [25]. The trabecular bone histology data described in the original study was provided in Tb. BV/TV (%), as this data was acquired through dynamic histomorphometry analysis (3D) [1]. Since ImageJ quantification provides 2D measurements, we reported our subset analysis data in area (mm^2). According to American Society for Bone and Mineral Research, volume ratios (3D) are considered numerically equivalent to area ratios (2D) [25].

2.2. Image acquisition

Histologic slides were photographed using a Keyence Fluorescence Microscope BZ-X700 (4× plan fluor PhL, Brightfield/Phase contrast) using an automated image capture software, BZ-X Analyzer, to create high resolution images. The images were exported as .tiff files prior to quantification/analysis of adipocytes. These images were also "image-stitched" with the BZ-X Analyzer software to produce a composite image of the entire slide (Fig. 1A).

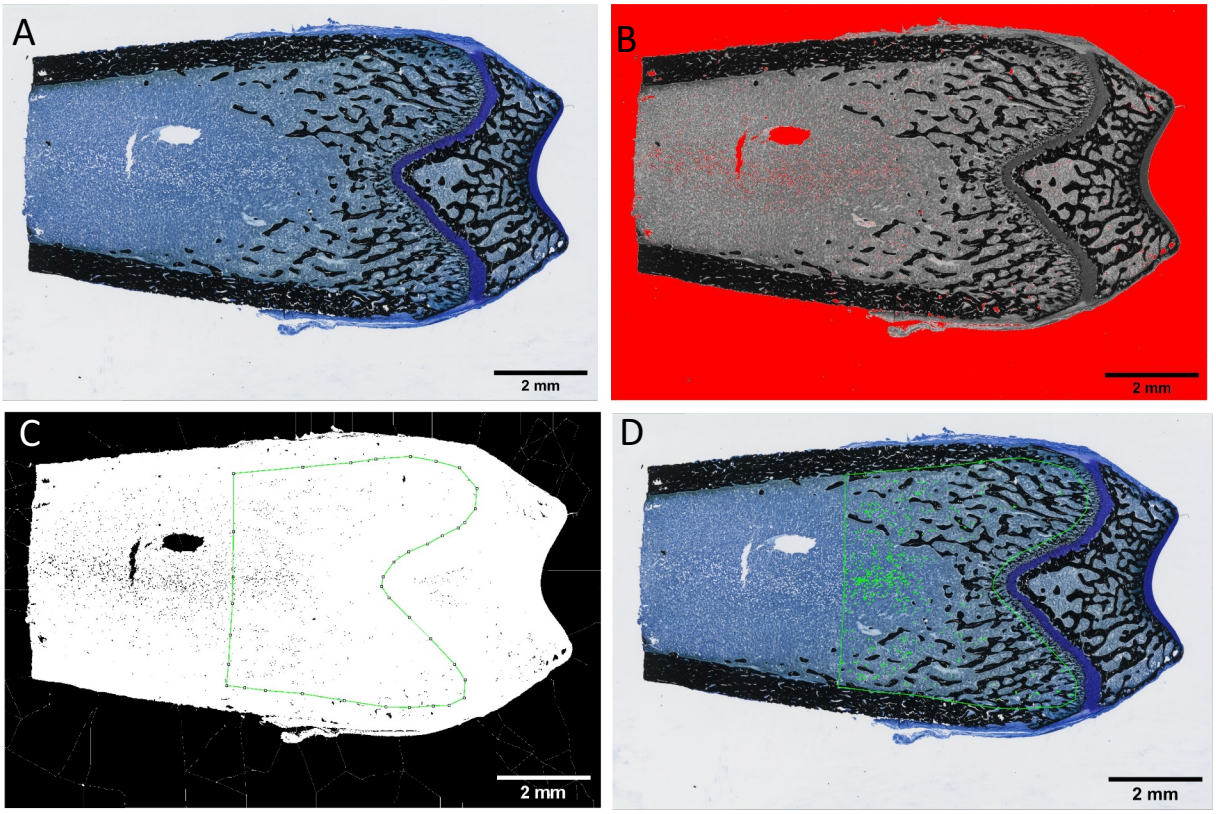

Fig. 1. Adipocyte quantification process of rat distal femoral metaphysis through ImageJ. (A) Original image and (B) image converted to 32-bit with *Huang* threshold filter at default thresholding with a dark background. Red highlight represents the areas that will be translated to black (255) value once the threshold is applied. (C) *Huang* threshold filter applied at the default level. The image had the plugins *Despeckle* and *Adjustable Watershed* applied and the marrow area is outlined with the ROI File (outlined in green). (D) Results from *Analyze Particles* measuring tool of the marrow area outlined by the ROI File that selected shapes based on specific parameters in size and circularity. The green overlay masks represent the counted adipocytes. (For interpretation of the references to color in this figure legend, the reader is referred to the web version of this article.)

2.3. Adipocyte parameter quantification and analysis

A blinded analysis of BM adipocytes was performed on each slide using ImageJ software (https://imagej.nih.gov/ij/) [26,27]. Treatment groups and sample numbers in this study are a subset analysis of the original study, and thus were not the primary endpoint used to power the original study, but were sufficient for our analysis and are shown here: 4-week treatments: Vehicle (n = 10/sex); Scl-Ab 3 mg/kg (n = 10/sex); Scl-Ab 50 mg/kg (n = 10/sex); and hPTH (male n = 8, female n = 10); 26-week treatments: Vehicle (n = 10/sex); Scl-Ab 3 mg/kg (n = 10/sex); Scl-Ab 50 mg/kg (n = 10/sex); and hPTH (n = 10/sex). A global scale was set at 530 pixels/mm based on the microscope imaging objective and settings. The tissue area (T.Ar) was selected in the distal femoral metaphysis (0.2 mm below the epiphyseal growth plate and 3 mm into the distal metaphysis) using the polygon tool to contain the BM and trabecular bone, excluding cortical bone. One histological slide per distal femur was measured. The T.Ar was measured using ImageJ to find the total tissue area, which was used to normalize adipocyte numbers per T.Ar for each image. The T.Ar selection was saved as an ROI (region of interest) file to ensure consistency within an image. Color images were converted to 32-bit and then thresholded using the *Huang* filter at the automatic level determined by ImageJ with dark background (Fig. 1B); red highlight represents the background (later excluded) and adipocyte areas that were translated to black once the threshold was applied [26,27]. [Note: thresholding an image converts it to black (255) and white (0) values [26,27], as shown in Fig. 1C]. Images were then processed with the *Despeckle* and *Adjustable Watershed* plugins (Fig. 1C). [*Despeckle* was used to automatically remove salt-and-pepper background noise that could cause inaccuracies with particle analysis, while the *Adjustable Watershed* ImageJ segmentation algorithm was used to systematically correct any adjacent adipocytes that had been merged into 1, back into 2 distinct objects. ImageJ typically applies a watershed segmentation threshold at a level of 0.5, but with the *Adjustable Watershed* the amount of segmentation can be changed to correct for closely packed adipocyte, tissue tears, or staining inconsistencies [26,27].] A blinded investigator set the *Adjustable Watershed* within the range of 0.3–0.8 to select the most appropriate segmentation threshold to apply to each image based solely on the quality of the individual image. Next, particle analysis for BM adipocytes was performed within the T.Ar by using the T.Ar ROI file and the *Analyze Particles* plugin. [This plugin scans a selected area and measures objects that meet parameters based on area and circularity [26,27]]. The particle circumference range was set to 40–400 pixels (area results displayed in mm^2 due to the set scale) and the circularity was set at 0.6–1.00 (1.00 being a perfect circle). These parameters were determined through an iterative, trial and error analysis of different images from different treatment groups until a universal measurement system was decided upon and then used for every image. After particle analysis, *Result* and *Summary* pop-up windows provided the average and total numbers of counted adipocytes and the area (mm^2) of the average adipocyte, within the T.Ar; these data were used to quantify adiposity in each sample. Average circumference measurements were calculated by estimating that the average adipocyte was a perfect circle. Yellow overlay masks identifying adipocytes summarized these data for visibility purposes (Fig. 1D). The original image, ROI selection, and yellow overlay mask of measured adipocytes were flattened into a singular image and saved as a .tiff file to preserve resolution quality.

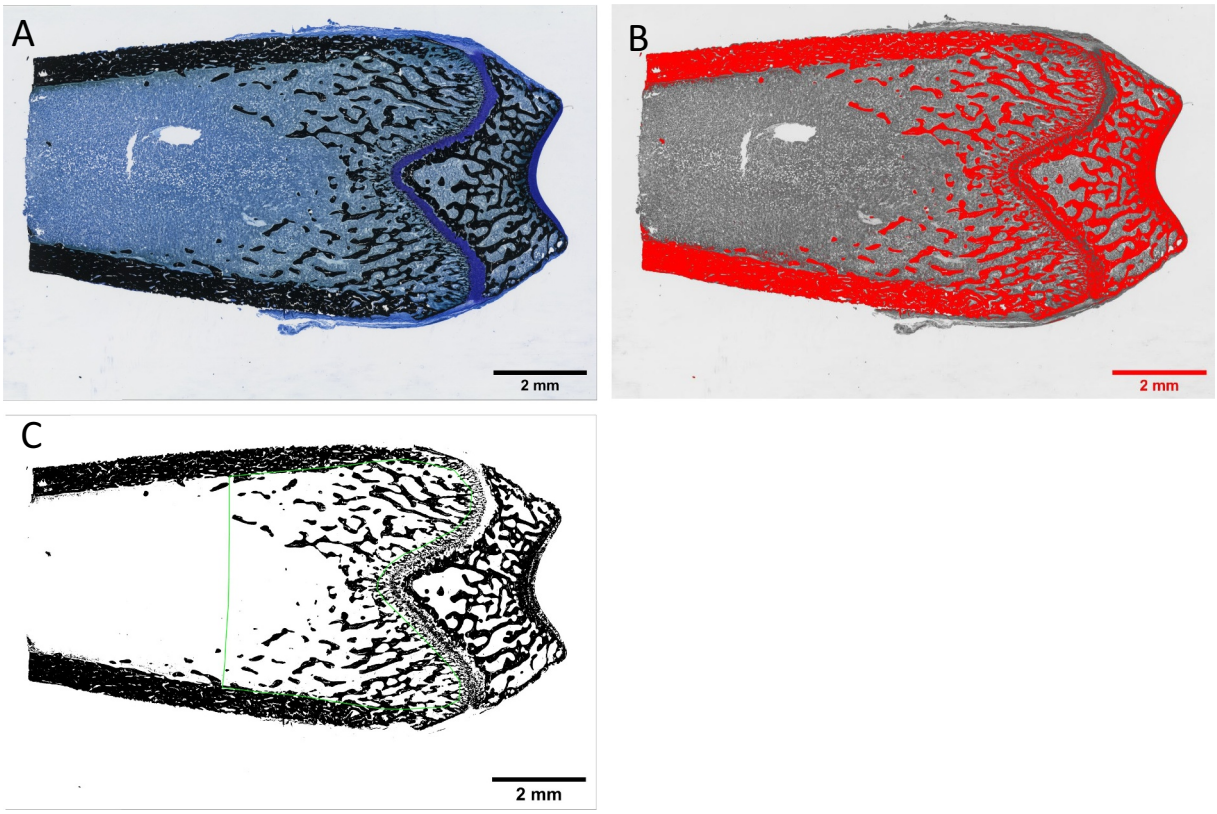

Fig. 2. Trabecular bone quantification of the bone marrow space in rat distal femoral metaphysis through ImageJ. (A) Original image and (B) image converted to 32-bit with *Huang* threshold that has been manually adjusted to only highlight for the trabecular bone. (C) The applied *Huang* threshold filter with the marrow area selected using the ROI (region of interest) File (outlined in green) so area and percent of trabecular bone space can be measured. (For interpretation of the references to color in this figure legend, the reader is referred to the web version of this article.)

2.4. Trabecular bone area quantification and analysis

Trabecular bone quantification was performed in ImageJ using the ROI file of the selected T.Ar to ensure the areas used to measure adipocytes, T.Ar, and trabecular bone were identical. As above, original images (Fig. 2A) were converted to 32-bit images and then *Huang* filter thresholded with a non-dark background [27,28]. The threshold was manually adjusted so only the trabecular bone was highlighted in red (Fig. 2B). Manual manipulation was used to refine any automatic thresholding inconsistencies that falsely labeled trabecular bone within the slide. With the T.Ar selected, the trabecular bone area was measured based on the threshold values represented in a binary scheme (Fig. 2C), (white = 0; black = 255 [26,27]). ImageJ provided the area (mm^2) and the percent area (%) of the black pixels within the T.Ar selection, which was recorded as trabecular bone area per tissue area (Tb. B.Ar/T.Ar).

2.5. Adipocyte quantification within the bone marrow space

After adipocyte analysis and quantification within the T.Ar (which includes the BM and trabecular bone) was used to quantify *tissue adiposity*, *marrow adiposity* was then calculated as the total adipose area within the marrow area (Ma.Ar) (which consisted of only BM). Trabecular bone area (mm^2) was subtracted from the total T.Ar (mm^2) to give the area of only the Ma.Ar (mm^2). The total adipocyte number and adiposity were then normalized to Ma.Ar to adjust for reduction in marrow space as a consequence of any increased B.Ar/T.Ar within the ROIs from osteoanabolic treatment.

2.6. Correlation analysis of trabecular bone area vs adipocyte number and adiposity

To determine if increased trabecular bone volume correlated with changes in BMAT, we then performed a linear correlation analysis between adipocyte number or adiposity (within the T.Ar and Ma.Ar) and Tb.B.Ar/T.Ar, which captures the total osteoblastic capacity (number and activity) during treatment durations for each treatment groups [4-week treatments: Vehicle (n = 10/sex); Scl-Ab 3 mg/kg (n = 10/sex); Scl-Ab 50 mg/kg (n = 10/sex); hPTH (male n = 8, female n = 10). 26-week treatments: Vehicle (n = 10/sex); Scl-Ab 3 mg/kg (n = 10/sex); Scl-Ab 50 mg/kg (n = 10/sex); hPTH (n = 10/sex)] of each sex (male and female) for both treatment durations (4-week and 26-week). The R^2 and slope of each linear regression test were measured to evaluate how closely the data fit along the linear regression line and the strength of the bone-BMAT relationship, respectively.

2.7. Statistical analysis

All data were graphed and analyzed using GraphPad Prism 7 software. Bar graphs represent mean ± S.E.M., unless otherwise stated. Statistical analyses were conducted between rat sexes, treatment groups, and treatment durations (4-week versus 26-week). When comparing treatment groups (Vehicle, Scl-Ab 3 mg/kg, Scl-Ab 50 mg/kg, and hPTH 75 μg/kg/d) across cohorts (either 4-week or 26-week; males or females), a 2-way ANOVA with Tukey's multiple comparison test was performed. When comparing differences over time (4-week versus 26-week) or between sex (male versus female), for the treatments (Vehicle, Scl-Ab 3 mg/kg, Scl-Ab 50 mg/kg, or hPTH) a 2-way ANOVA with Sidak's multiple comparison test was performed. Significance was defined as $p < 0.05$: *$p < 0.05$ vs. Vehicle; $^{h}p <$

0.05 vs. hPTH; $^{T}p < 0.05$, 4-week vs. 26-week; $^{A}p < 0.05$ Scl-Ab (3 mg/kg) vs. Scl-Ab (50 mg/kg); $^{S}p < 0.05$ Male vs. Female. Statistical analyses were conducted for correlations using an XY linear regression test with 95% confidence, and significance was defined as: *p < 0.05, **p < 0.01, ***p < 0.001, ****p < 0.0001.

3. Results

3.1. ImageJ validation

We first compared our ImageJ-based adipocyte quantification method to an OsteoMeasure software-based method using distal femoral metaphysis bones of female mice fed a control diet (n = 5) or a rosigliatzone-supplemented diet (n = 5) for four weeks (Supplemental Methods and Supplemental Fig. 1A, B) using similar methods and adipocyte parameters as previously stated in Section 2.3. The ImageJ data was then compared to adipocyte quantification data provided through OsteoMeasure Image software (OsteoMetrics, Atlanta, GA, USA) on the same subset of femurs in the same ROIs. We observed no significant differences between the measured adiposity of the control groups and no significant difference between total adiposity of the rosiglitazone-supplemental groups when comparing the two different analysis methods (Supplemental Fig. 1C). Both, ImageJ and OsteoMeasure resulted in the same significance ($p < 0.0001$) when comparing BM adiposity between the control and rosiglitazone-supplemented groups (Supplemental Fig. 1C).

3.2. Osteoanabolic treatments generally decrease BMAT in male and female rats

After validating our ImageJ-based analysis method, we proceeded to assess BMAT in the rat bones of interest. Surprisingly, Scl-Ab treatments had a significantly positive effect on tissue adiposity after 4-week treatments in females, although this was reversed by 26 weeks, as discussed below (Table 1, Fig. 3A–C). The 4-week Scl-Ab (50 mg/kg) group was also significantly higher in adipocyte number and tissue adiposity when compared to hPTH treatments (Fig. 3A, C). Females after 4 weeks of treatment illustrated no significant difference in adipocyte circumference when compared to the vehicle treated group (Fig. 3B). In contrast to females, 4-week treated males experienced a nonsignificant negative trend in tissue adiposity for all treatment groups (Table 1, Fig. 3D–F). Also surprisingly, males also displayed a significant increase in adipocyte circumference with 4-week hPTH treatments when compared to the vehicle treatment group (Fig. 3E).

As expected, after 26 weeks of treatment, Scl-Ab and hPTH reduced tissue adiposity relative to the vehicle-treated in both males and females (Table 1). For females, Scl-Ab (50 mg/kg) and hPTH significantly decreased adipocyte number and tissue adiposity after 26 weeks of treatment when compared to the vehicle-treated (Fig. 3A, C). Scl-Ab (50 mg/kg) also significantly reduced adipocyte number tissue adiposity when compared to Scl-Ab (3 mg/kg) at 26 weeks and when compared to Scl-Ab (50 mg/kg) after 4 weeks, demonstrating dose- and time-dependence (Fig. 3A, C). Females displayed a nonsignificant decrease in adipocyte circumference at 26 weeks (Fig. 3B).

In males, tissue adiposity and adipocyte number (but not adipocyte circumference) showed significant, large negative responses to all treatment groups versus the vehicle-treated group after 26 weeks (Fig. 3D–F). Scl-Ab did not display a dose-dependent variation in adipocyte number or tissue adiposity like seen in the females (Fig. 3D, F). The 26-week Scl-Ab (3 mg/kg) group displayed a significant increase in tissue adiposity when compared to the corresponding 4-week group, indicating that age-driven adipogenesis occurred in this group, although to a lesser extent than seen in the vehicle-treated group (Fig. 3F). hPTH in males, in contrast to females, had significantly decreased adipocyte circumference over time (from 4-week to 26-week) (Fig. 3E).

The 26-week vehicle-treated females had a significant increase in tissue adiposity and adipocyte number compared to the 4-week vehicle-treated (Fig. 3A, C), and nonsignificant differences in adipocyte circumference (Fig. 3B). Vehicle-treated males showed a significant increase in adipocyte number and tissue adiposity after 26 weeks compared to the 4-week time point, indicating age-dependent BM adipogenesis (Fig. 3D, F). In summary, both males and females had increased tissue adiposity after 26 weeks for the vehicle-treated groups. Both sexes also demonstrated greater negative effects on BMAT after longer administration times of the osteoanabolic agents. Scl-Ab displayed dose and time dependent factors that affected adipocyte number and tissue adiposity for both sexes when looking within the total tissue area.

3.3. Significant differences between males and females were observed in vehicle and treated groups

To further explore sex differences, we re-analyzed the data with regard to sex rather than time point and dose-dependency within the T.Ar (Fig. 3G–L). After 4 weeks of treatment the vehicle-treated females had significantly lower adipocyte number and tissue adiposity (Fig. 3G, I) than males, which may explain why Scl-Ab had differing effects on adiposity after 4 weeks of treatment in the two sexes. A significant sex variation was also observed in males versus females treated with hPTH

Table 1
Comparative results of trabecular bone area (Tb. B.Ar/T.Ar, %) and adiposity (%) within the tissue area (T.Ar) of male and female distal rat femurs treated with Scl-Ab (3 mg/kg and 50 mg/kg) and hPTH (75 μg/kg/d) relative to the vehicle-treated groups (Treatment group/Vehicle) after 4 and 26 weeks of treatment. Data for Tb. B.Ar/T.Ar (%) and Tissue adiposity (%) shown as mean ± S.E.M. *p < 0.05 vs. Vehicle.

		Week 4				Week 26			
		Tb. B.Ar/T.Ar (%)	Tb. B.Ar/T.Ar Relative to Vehicle	Tissue Adiposity (%)	Tissue Adiposity Relative to Vehicle	Tb. B.Ar/T.Ar (%)	Tb. B.Ar/T.Ar Relative to Vehicle	Tissue Adiposity (%)	Tissue Adiposity Relative to Vehicle
Males	Vehicle	21.485	1.000	1.308	1.000	23.531	1.000	2.906	1.000
	Scl-Ab 3 mg/kg	28.456	1.324	1.025	0.784	38.523*	1.637	1.797*	0.618
	Scl-Ab 50 mg/kg	25.922	1.206	1.066	0.815	55.245*	2.348	1.357*	0.467
	hPTH	43.386*	2.019	0.936	0.716	63.542*	2.700	0.796*	0.274
Females	Vehicle	34.475	1.000	0.613	1.000	38.825	1.000	1.203	1.000
	Scl-Ab 3 mg/kg	38.515	1.117	1.123*	1.834	49.664*	1.279	1.087	0.903
	Scl-Ab 50 mg/kg	43.152*	1.252	1.288*	2.102	72.555*	1.869	0.545*	0.453
	hPTH	43.649*	1.266	0.685	1.118	57.766*	1.488	0.555*	0.461

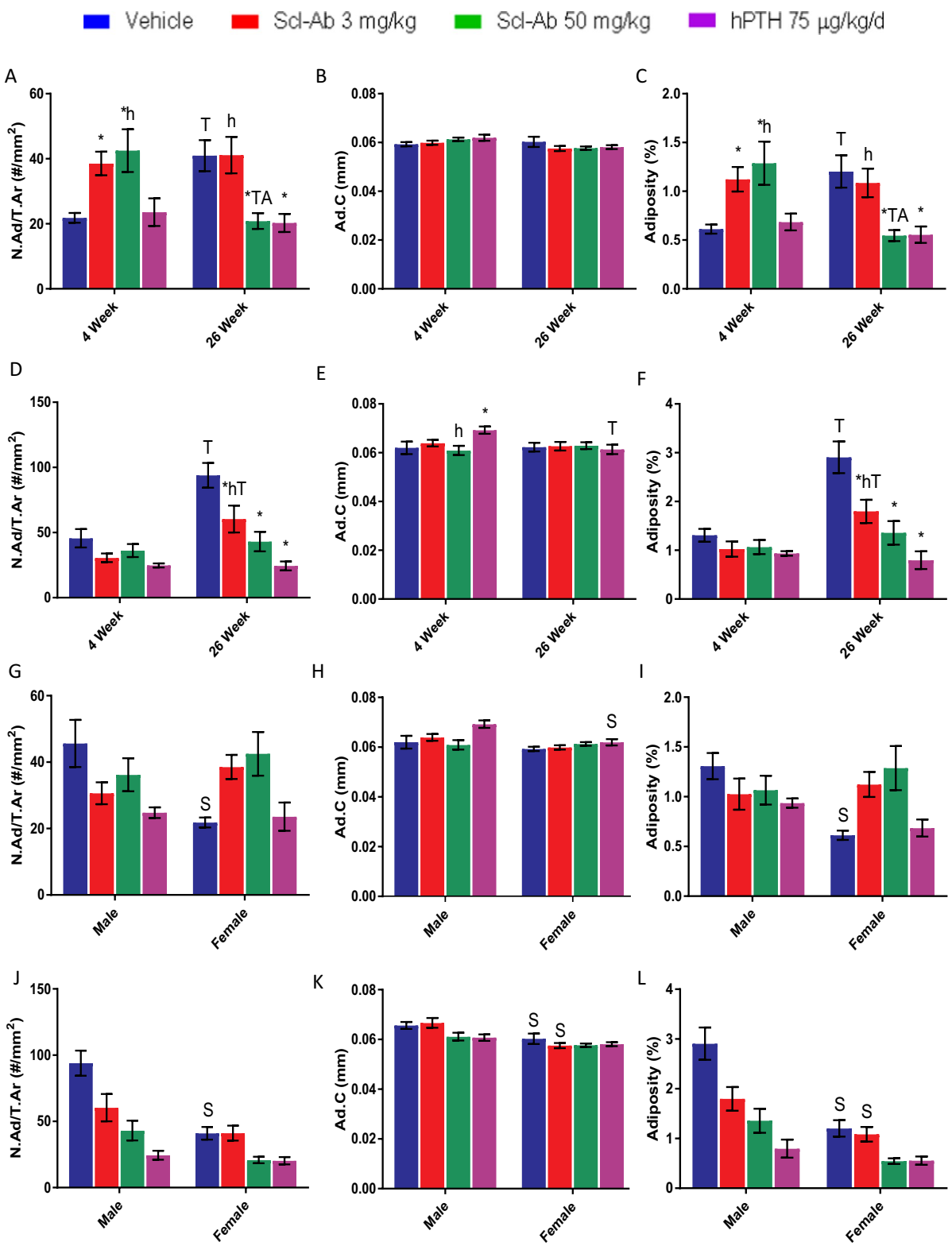

Fig. 3. Effects of Scl-Ab (3 mg/kg or 50 mg/kg) and hPTH (75 µg/kg/d) on adipocyte number per tissue area (N.Ad/T.Ar), average adipocyte circumference (Ad.C), and tissue adiposity (%) [Calculated as: (N.Ad* Average Adipocyte Area)/T.Ar] in male and female distal rat femurs after the 4-week and 26-week treatments (A) Adipocyte number per tissue area in females. (B) Average adipocyte circumference in females. (C) Female tissue adiposity. (D) Adipocyte number per tissue area in males. (E) Average adipocyte circumference in males. (F) Male tissue adiposity. (G) Adipocyte number per tissue area for 4-week male and female. (H) 4-week male and female adipocyte circumference. (I) 4-week male and female tissue adiposity. (J) Adipocyte number per tissue area in 26-weeks male and female. (K) 26-week male and female average adipocyte circumference. (L) 26-week male and female tissue adiposity. *$p < 0.05$ vs. Vehicle; $^{h}p < 0.05$ vs. hPTH; $^{T}p < 0.05$, 4-week vs. 26-week; $^{A}p < 0.05$ Scl-Ab (3 mg/kg) vs. Scl-Ab (50 mg/kg); $^{S}p < 0.05$ Male vs. Female. Data shown as mean ± S.E.M. All analyses were performed as 2-way ANOVA + Tukey's/Sidak's multiple comparison tests within Prism. **Abbreviations**: Ma.Ar = marrow area, in mm^2. Tb. B.Ar = trabecular bone area, in mm^2. T.Ar = tissue area [calculated as trabecular bone area + marrow area (Tb. B.Ar + Ma.Ar)], in mm^2. All measurements and ROIs exclude cortical bone.

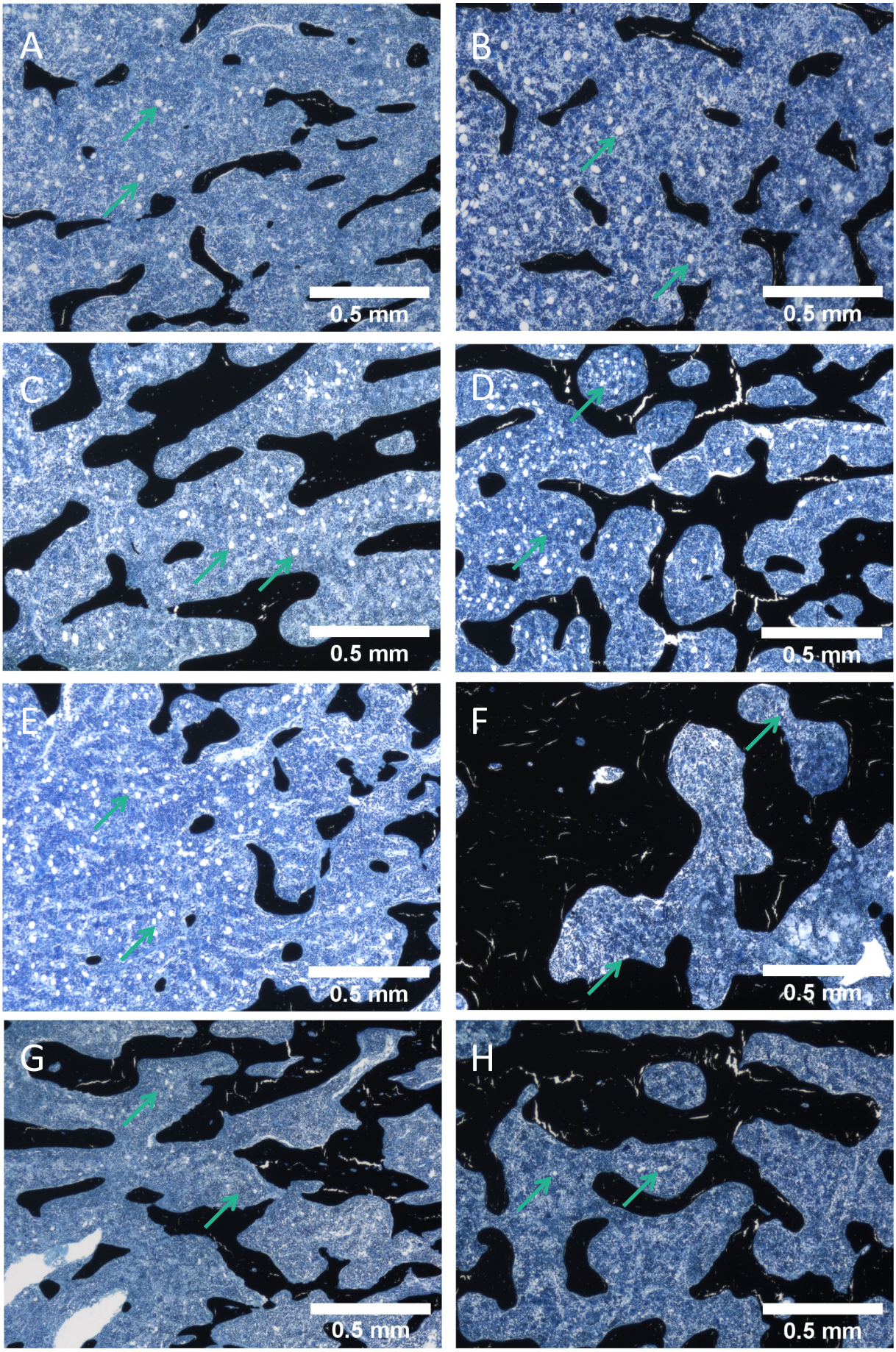

(caption on next page)

Fig. 4. Representative images of Von Kossa tetrachrome-stained female rat distal femur metaphysis slides. Exemplify adipose tissue (green arrows) modification and trabecular bone acquisition within the bone tissue area of each treatment group for the rats at 4-week vs 26-week. (A, C, E, G) 4-week females treated with Vehicle, Scl-Ab 3 mg/kg, Scl-Ab 50 mg/kg, and hPTH, respectively. (B, D, F, H) 26-week females treated with Vehicle, Scl-Ab 3 mg/kg, Scl-Ab 50 mg/kg, and hPTH, respectively. These images were generated as individual images during the image stitching process via the Keyence BZ-X700 Microscope. (For interpretation of the references to color in this figure legend, the reader is referred to the web version of this article.)

in regards to adipocyte circumference (Fig. 3H).

The trend between male and female vehicle-treated groups was again observed at 26-weeks, where males had significantly more adipocytes and overall tissue adiposity than females, but after 26 weeks females also had significantly smaller adipocyte circumference (Fig. 3J–L). Adipocyte circumference and tissue adiposity were also significantly decreased in females versus males in Scl-Ab (3 mg/kg) and vehicle groups at the 26-week time point (Fig. 3K, L).

3.4. Effects of Scl-Ab and hPTH on trabecular bone are sex, time, and dose-dependent

To better understand the trabecular bone-BMAT relationship, we next analyzed trabecular bone area changes within the same subset of rat histology slides and ROIs as above, using our ImageJ-based method for trabecular bone area/tissue area quantification. After 4 weeks of Scl-Ab (50 mg/kg) and hPTH, female rats showed significant increases in bone area (Supplemental Table 1, Supplemental Fig. 2A). As predicted, by 26 weeks females showed significant increases in trabecular bone mass when compared to 26-week vehicle-treated females for all the treatment groups, and when compared to their corresponding 4-week treatment group (Supplemental Fig. 2A).

Males, similarly to females, had significantly more trabecular bone after the 4-week hPTH treatment compared to vehicle group, but contrary to females, also had more bone in the hPTH versus Scl-Ab (3 mg/kg and 50 mg/kg) groups at this time point (Supplemental Table 1, Supplemental Fig. 2B). However, similar to females, after 26 weeks of treatment, males exhibited significant increases in trabecular bone area in all treatment groups compared to the vehicle-treated group, and compared to the corresponding 4-week treatments (Supplemental Fig. 2B). Scl-Ab (50 mg/kg) induced a more significant and greater fold increase in trabecular bone mass than Scl-Ab (3 mg/kg), indicative of dose-dependency after chronic drug administration in males and females (Supplemental Table 1, Supplemental Fig. 2A, B). Overall, our reanalysis from a subset of histology samples of the trabecular bone from the rat distal femoral metaphysis proved to be consistent with the full set data analysis for distal femur published by Ominsky et al. [1] (reproduced in Supplemental Fig. 3).

As illustrated in our prior data, females had lower baseline adipocyte parameters within the T.Ar (Fig. 3G, I, J, L) than males; female rats also had statistically more trabecular bone than their male counterparts at the 4-week and 26-week time points (Supplemental Table 1, Supplemental Fig. 2C, D). After 4 weeks and 26 weeks of treatment with Scl-Ab (3 mg/kg and 50 mg/kg) the trabecular bone in females was significantly higher than in males of the same treatment groups (Supplemental Fig. 2C, D). However, after 4 weeks and 26 weeks hPTH demonstrated no sex differences, in accordance with our finding that hPTH treatments induced a stronger effect on males (2.019 fold increase at 4 weeks, 2.700 fold increase at 26 weeks) than females (1.266 fold increase at 4 weeks, 1.488 fold increase at 26 weeks) when compared to the vehicle treated group (Supplemental Table 2, Supplemental Fig. 2C, D). Thus, there are sex-based differences in the initial amount of trabecular bone in rats and how each sex responds to osteoanabolic agents.

3.5. Trabecular bone volume inversely correlates with BMAT within the tissue area

To compare how BM adiposity (normalized to the T.Ar) correlated with trabecular bone area within the overall tissue area, we performed a linear regression analysis using BM parameters of adipocyte number, circumference, and overall tissue adiposity against Tb. B.Ar/T.Ar. After the 4-week treatments, females showed a trend for inverse correlations between adipocyte number and Tb. B.Ar/T.Ar, and for tissue adiposity and Tb. B.Ar/T.Ar (Supplemental Fig. 4A, C). Surprisingly, females demonstrated a significant direct correlation between adipocyte circumference and trabecular bone area ($p < 0.0005$) (Supplemental Fig. 4B). Males showed a similar pattern with a significant inverse correlation after 4 weeks of treatment between adipocyte number and bone area ($p = 0.0037$) as well as tissue adiposity and bone area ($p = 0.0213$) and a surprising significant positive correlation with adipocyte circumference ($p < 0.0001$) (Supplemental Fig. 4D–F).

By 26 weeks, females and males showed a significant inverse correlations between trabecular bone area and adipocyte number as well as trabecular bone area and tissue adiposity, and no significant correlations between adipocyte circumference and trabecular bone area (Supplemental Fig. 4G–L). For both males and females, adipocyte number and tissue adiposity correlations with trabecular bone area became stronger over time (Supplemental Fig. 4). Ultimately, when normalizing to the T.Ar, these data indicate that Tb. B.Ar/T.Ar is significantly and inversely correlated with BM adipose tissue after short-term treatment (for males only) and after chronic treatment for both sexes. Thus, these data indicate that osteoanabolic agents increase bone while decreasing adiposity mainly through affecting number rather than size of adipocytes, which suggests that adipogenesis or mature adipocyte survival may be affected by these agents, although our analysis methods do not allow us to determine this conclusively.

3.6. Short-term Scl-Ab treatments significantly increased marrow adiposity and adipocyte number within the marrow area in females

Results in Fig. 3 and Supplemental Fig. 4 could be partially explained by changes in bone volume and medullary space for adipocytes to reside, rather than true changes in adiposity; to account for this, we performed a final analysis normalizing adiposity to marrow area (Ma.Ar, defined as tissue area (T.Ar) minus trabecular bone area (Tb. B.Ar)) rather than whole T.Ar to account for the change in marrow area, independent of bone. When looking at adipocyte number and marrow adiposity normalized to the Ma.Ar, females showed a significant increase with Scl-Ab (3 mg/kg and 50 mg/kg) relative to the vehicle-treated after 4 weeks (1.974 and 2.397 fold change, respectively) (Supplemental Table 2, Supplemental Fig. 5A, C). After chronic treatment, hPTH showed a nonsignificant decreasing trend in marrow and the increase in adiposity from Scl-Ab seen at 4 weeks was lost in females' adiposity (Supplemental Table 2, Supplemental Fig. 5C). Comparing these results to effects of the agents when normalizing adiposity to the larger T.Ar, it is clear that many of the previously identified significant changes were due to reductions in bone marrow space as a result of increased bone area rather than effects on adipocytes specifically in the marrow cavity. Representative images taken from the distal femoral metaphysis support this quantification at 4 and 26 weeks in females (Fig. 4, whole sample images in Supplemental Fig. 7).

3.7. Chronic hPTH treatments caused a reduction in marrow adiposity and adipocyte number within the marrow area in males

After 4 weeks of treatment, males showed no significant differences in adipocyte number or marrow adiposity per Ma.Ar, between any of

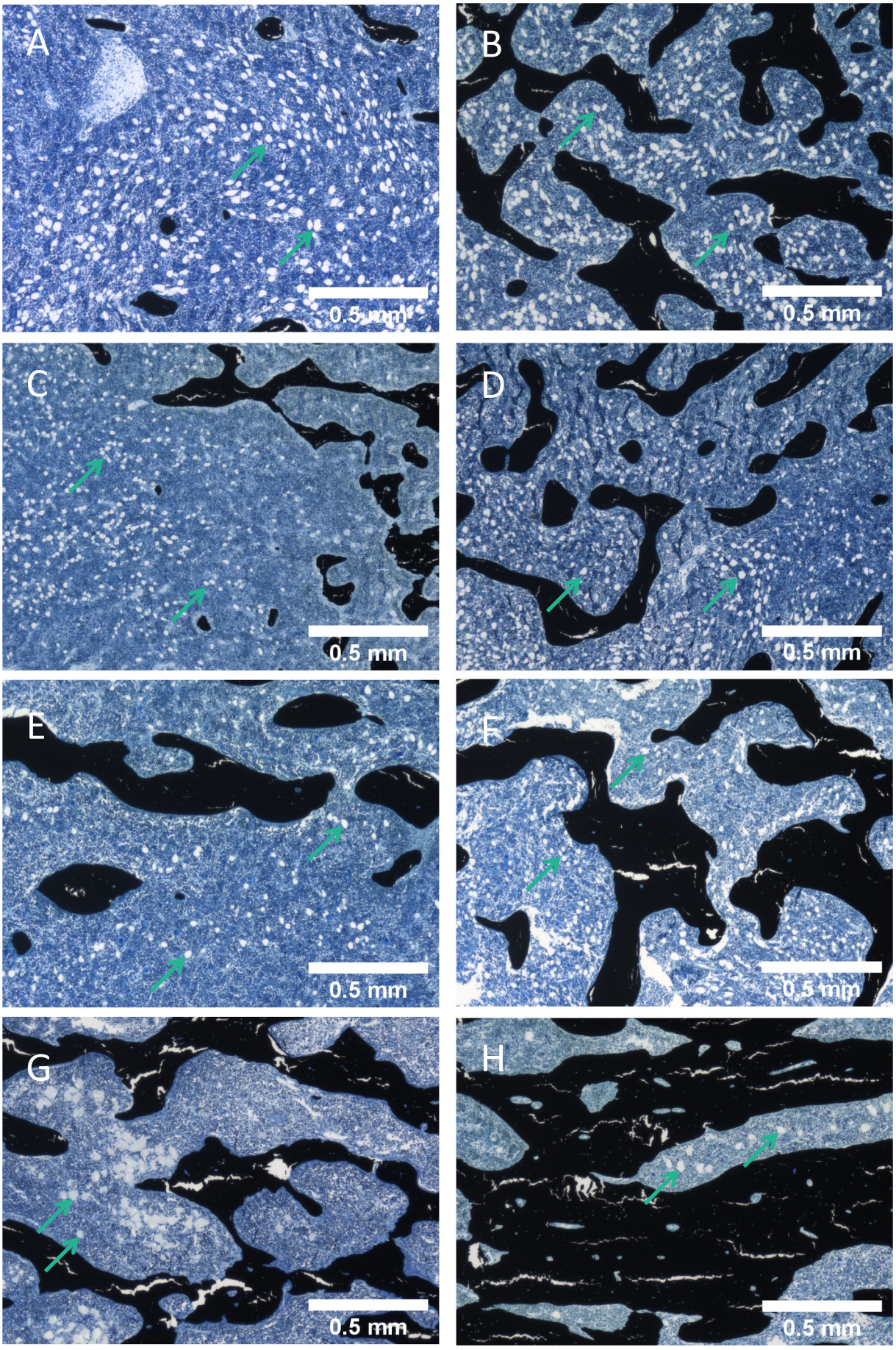

(caption on next page)

Fig. 5. Representative images of Von Kossa tetrachrome-stained male rat distal femur metaphysis slides. Exemplify adipose tissue (green arrows) modification and trabecular bone acquisition within the bone tissue area of each treatment group for the rats at 4-week vs 26-week. (A, C, E, G) 4-week males treated with Vehicle, Scl-Ab 3 mg/kg, Scl-Ab 50 mg/kg, and hPTH, respectively. (B, D, F, H) 26-week males treated Vehicle, Scl-Ab 3 mg/kg, Scl-Ab 50 mg/kg, and hPTH, respectively. These images were generated as individual images during the image stitching process via the Keyence BZ-X700 Microscope. (For interpretation of the references to color in this figure legend, the reader is referred to the web version of this article.)

the treatments and the vehicle (Supplemental Table 2, Supplemental Fig. 5D, F). After 26-weeks, vehicle-treated males showed a significant increase in adipocyte number and marrow adiposity compared to the 4-week time point, indicative of age related BM adipogenesis (Supplemental Fig. 5D, F). hPTH significantly decreased adipocyte number and adiposity per Ma.Ar after chronic treatment compared to the vehicle (0.584 fold change), indicating chronic hPTH treatments overcame aging-induced adipogenesis (Supplemental Table 2, Supplemental Fig. 5D, F). Scl-Ab (3 mg/kg and 50 mg/kg) showed a significant increase in adipocyte number and marrow adiposity over-time when comparing the 26-week treatment to the corresponding 4-week group (Supplemental Fig. 5D, F), indicating that these treatments did not completely overcome aging-induced adipogenesis. Chronic hPTH in males resulted in a significant decrease in adipocyte circumference from the 4-week to 26-week treatment group (Supplemental Fig. 5E). Representative images taken from within the distal femoral metaphysis of males support this quantification at 4 and 26 weeks (Fig. 5, whole sample images in Supplemental Fig. 8).

3.8. Baseline adipocyte parameters and drug responses per marrow area vary by sex

Similar to the sex differences seen within the T.Ar, after 4 weeks vehicle-treated males had significantly more adipocytes and more overall adiposity per Ma.Ar than females (Supplemental Fig. 5G, I). While 4-week Scl-Ab (50 mg/kg)-treated females had significantly more adipocytes and marrow adiposity than males (Supplemental Fig. 5G, I). After chronic administration, the same sex variance was seen within the vehicle treated groups with males having more adipocytes and marrow adiposity than females (Supplemental Fig. 5J, L).

3.9. Trabecular bone area correlations with BMAT quantified within the marrow area are similar but not identical to correlations with BMAT quantified within the total area

After our linear regression analysis of BMAT normalized to the T.Ar, we re-analyzed the relationship of BMAT normalized to Ma.Ar versus Tb. B.Ar/T.Ar to investigate if these correlations were the same or different. Overall, we found less significant correlation between BMAT and bone when analyzing BMAT using Ma.Ar instead of T.Ar. Similar to the prior correlation analysis, females showed no significant correlations with adipocyte number versus trabecular bone area or marrow adiposity versus trabecular bone area, but illustrated a significant direct correlation ($p = 0.0005$) for adipocyte circumference versus trabecular bone area after 4 weeks of treatment (Supplemental Fig. 6A–C). After 4 weeks, males showed a significant inverse correlation for adipocyte number ($p = 0.0171$), yet a significant direct correlation for adipocyte circumference ($p < 0.0001$) versus trabecular bone area (Supplemental Fig. 6D–F), and overall less significance than seen with the prior correlation analysis (Supplemental Fig. 4D–F). By 26 weeks of treatment, females showed no significant correlations between Tb. B.Ar/T.Ar and any of the BMAT parameters (Supplemental Fig. 6G–I), contrasting the correlation results of Supplemental Fig. 4G, I. Males after 26 weeks maintained the significant inverse correlation between adipocyte number and trabecular bone area ($p = 0.0416$) (Supplemental Fig. 6J–L), although lost the previously identified negative correlation between adiposity and trabecular bone. Overall, these data suggest that by calculating adiposity as adipose area per total area rather than adipose area per marrow area inflates changes in adiposity measurements by inherently including changes in bone within the calculation.

4. Discussion

Through our novel ImageJ adipocyte and trabecular bone quantification method, we demonstrated that osteoanabolic agents (Scl-Ab and hPTH) favor bone acquisition, often at the expense of adipocytes, by exploring the correlation between trabecular bone area and bone marrow adipose tissue in a dual area analysis of rat bones. These findings align well with other data that bone cells directly regulate BMAT and that BMAT can reciprocally regulate bone mass accrual [2]. This cyclic relationship may indicate that the results of this study also highlight the differences between the overall tissue area and marrow area within the bone cavity and how normalizing adiposity to these two areas alter our understanding of the bone-BMAT relationship. MSC fate decisions (i.e. osteoblast or adipocyte differentiation) likely depend on the requirements and signals from adipocytes and osteoblasts in the BM microenvironment, although the exact relationship between osteoblasts, adipocytes and their progenitors is currently still under investigation. Our results illustrate that the inverse correlations between bone and BMAT in male and female rats is dependent on whether BMAT is normalized to the total tissue area (representative of the overall bone marrow cavity) or to total non-mineralized marrow area (representative of the hematopoietic and adipose tissue niche). For example, the inverse relationship between adipocyte number per marrow area and bone volume in male rats after 4 and 26 weeks of treatments (Supplemental Fig. 6D, J) may be due either to signaling between osteoblasts/osteocytes and adipocytes or their progenitors, direct effects of the osteoanabolic agents on the adipocyte lineage, or other mechanisms, but is not exclusively due to a competition for space. Similarly, Supplemental Fig. 4I and L, showed after 26 weeks of osteoanabolic treatments there were significant inverse correlations ($p < 0.0001$) between tissue adiposity and trabecular bone area in both sexes. However, Supplemental Fig. 6I and L illustrated no inverse correlations between marrow adiposity and trabecular bone area for either sex; thus, the significant decrease in adiposity with increase in bone could be considered artificially inflated because of the decreased space for adipocytes resulting from increased bone measurements, rather than any effect on the adipocytes specifically. Similarly, as seen in Fig. 3C,F, chronic Scl-Ab treatments had significant decreases in adipocyte number and tissue adiposity (when normalized to T.Ar) and displayed dose- and time-dependent factors. However, Supplemental Fig. 5C,F showed Scl-Ab having nonsignificant changes in marrow adiposity (when normalized to Ma.Ar) compared to vehicle; this again suggests that reductions in the available bone marrow space due to increased bone accrual caused the observed decrease in T.Ar adiposity rather than Scl-Ab having a direct negative effect on adiposity in the marrow cavity, independent of bone changes.

This work also describes a new, systematic approach using free software to quantifying BM adipocytes and trabecular bone that could be of great use to bone researchers worldwide. Our ImageJ method provides researchers the ability to perform an unbiased adipocyte analysis on previously-stained samples, or samples that were not originally prepared for any form of adipocyte analysis, and normalizes to either total tissue area or marrow area exclusive of bone. As this study was a re-analysis of a subset of samples obtained from a prior experiment, marrow adiposity was not the primary outcome, but the samples still proved useful in making novel discoveries about the BMAT-bone

connection. This demonstrates that this novel method allows researchers to re-analyze histology samples from prior experiments and hence obtain new information from previous studies, or provide opportunities for future collaborations.

The observed differences in adiposity and trabecular bone area between the age-matched male and female rats in this study at baseline and in response to treatment (within the tissue area and marrow area) are intriguing and represent an avenue that needs more exploration. The 4 and 26-week vehicle-treated female rats had lower adipocyte numbers and less overall bone marrow adiposity than their male counterparts. Female rats have been observed to reach skeletal and sexual maturity sooner than males. At the time female growth attenuates, males continue to grow and accrue skeletal mass [29,30]. Female rats, like women, may experience fluctuations in hPTH levels, or higher hPTH levels earlier in life, that potentially cause increased bone acquisition earlier than males, which may be related to estrogen signaling as well [31–33]. Estrogen has anti-resorption properties that work to preserve trabeculae resulting in increased trabecular bone mass, especially in the primary spongiosa [34]. We postulate these hormonal differences may tip the scale in favor of osteogenesis at the expense of BMAT, as seen with the vehicle-treated females. However, without serum data to support the role sexual steroids played in the bone-BMAT relationship, explanations for the observed sex differences are only speculative.

Postmenopausal osteoporosis patients present with low bone density associated with high bone marrow adiposity [35]. Raloxifene, a selective estrogen receptor modulator (tissue-specific estrogen agonist), is an osteoporosis therapy that specifically relies on the anti-resorption effects of estrogen to increase bone mineral density [35–37]. Beekman et al. showed that after two years of raloxifene treatments (60 mg/kg and 120 mg/kg), women with postmenopausal osteoporosis had no significant changes to bone marrow adiposity, adipocyte number, or adipocyte size when compared to the placebo group, which contrasts the decreases in T.Ar BMAT parameters we observed in response to chronic Scl-Ab and hPTH treatments in male and female rats. [35,37]. Beekman et al. also demonstrated that high BM adiposity associated with large adipocyte size can lead to vertebral fractures in osteoporotic patients, indicating that adipocyte size may affect overall bone structure and quality [35]. On the other hand, risedronate, a bisphosphonate, functions mainly by inhibiting osteoclast activity, and also by promoting osteoblastogenesis; it has been shown to reduce bone marrow adipogenesis [38,39]. Duque et al. showed that after three years of risedronate treatments, postmenopausal women had significantly reduced *PPARγ* expression within the bone marrow of transiliac bone biopsies [38]. The risedronate-treated group also showed significantly-reduced adipocyte volume and adipocyte number per tissue volume, but adipocyte diameter remained unchanged compared to placebo [38,39], which aligns with the effects we observed after chronic Scl-Ab (only Scl-Ab 50 mg/kg in females) and hPTH treatments in both sexes within the T.Ar. Overall, both raloxifene and risodronate have been reported to increase bone mineral density [35–37,40] similar to the effects we observed with hPTH and Scl-Abs in rats. Differences in life stage/aging, species, or osteoanabolic mechanism may explain the difference in BMAT response to these and other osteoanabolic treatments.

In a sclerostin-knockout (SOST-KO) mouse model, we previously observed significant increases in overall bone volume and decreases in BMAT in the proximal and distal tibia compared to wild-type mice [2]. Administration of Scl-Ab to wild-type mice also showed increased Tb.B.Ar/T.Ar and decreased BMAT (significantly fewer and smaller adipocytes) within the T.Ar of tibia and femur [2]. Similarly, within the T.Ar of our male and female rats, the adipocyte number significantly decreased with chronic administration of high dose Scl-Ab, although adipocyte size remained unchanged (Fig. 3A, B, D, E). The decrease in adipocyte number was the driving factor in decreased tissue adiposity (Fig. 3C, F) and drove the inverse correlations between bone and adiposity seen at 26 weeks in male and female rats (Supplemental Fig. 4I, L). Overall, the changes in adipocyte number seen in the genetic model, the Scl-Ab mouse model, and our rat femur models demonstrate that sclerostin may play a functional role in adipogenesis or survival of mature adipocytes; lineage-tracing models would help to untangle these different explanations for our observations [2].

Like sclerostin, hPTH also regulates the bone-BMAT balance; a relationship which was recently elucidated in human cells and mice [23,24]. Specifically, Lanske et al. confirmed the ability for hPTH to decrease adipogenesis by genetically deleting PTHR1 from Prx1-expressing cells, and observed that this induced high BMAT and a doubling of the Pref1^{+}RANKL^{+} marrow progenitor cells [23]. Kronenberg et al. further confirmed this using deletion of PTHR1 in Sox9-cre progenitors [24]. Similar effects of hPTH on adipogenesis have been previously reported in rat ovariectomy models [41] and in vitro [42]. In male rats, chronic hPTH treatments appeared to have a direct effect on adipocyte differentiation or survival due to the significant decrease in adipocyte number and adiposity within the T.Ar and Ma.Ar (Fig. 3D, F and Supplemental Fig. 5D, F). Together these studies demonstrate that bone marrow MSCs and/or mature adipocytes are responsive to both sclerostin and hPTH, and suggest that these therapies may skew MSC fate. Because specific interrogation of adipocyte progenitor cells, which may or may not be the same as the bone lining cells described in the original manuscript, is necessary to determine the causes of BMAT changes, future research should be directed at testing effects of bone anabolic agents on adipocyte progenitor cells. It is possible that Scl-Ab and hPTH provide two distinct mechanisms whereby marrow progenitors are signaled to differentiate down the osteogenic lineage, but it is also known that both converge by stimulating the Wnt signaling pathway [20]. Further research is required to definitively demonstrate that Scl-Ab and hPTH treatments favor pre-osteoblast/osteoblast formation over adipogenesis in MSC progenitors in a complex microenvironment and test the amount of pathway convergence through which these treatments act.

One major question that remains in this study and the field in general, is where BM adipocytes originate from and why there were less of these cells after long-term osteoanabolic treatment. The observed changes in adipocyte number and circumference suggest effects on both mature adipocytes (such as delipidation, lipolysis, or apoptosis) and on the process of adipogenesis. Although the exact population of pre-adipocyte progenitor cells is still under investigation, it is suggested that there are distinct progenitor pools located throughout the bone cavity [1]. As previously investigated within the larger female cohort from this study, RUNX2-positive peritrabecular osteoprogenitors (one cell layer from the bone surface) and RUNX2-postive marrow osteoprogenitors (within the marrow, adjacent to marrow vessels) were decreased with Scl-Ab and hPTH treatments in a time and dose-dependent manner [1]. Thus, the decrease in adipocytes observed here may be in part due to a decrease in their progenitor cells. As the authors point out, a proliferation marker analysis was not performed, making this an imperfect assessment of MSCs.

In sum, we have assessed changes related to bone marrow adipocyte size and number in the marrow microenvironment; this method may be useful in addition to other types of analysis, to gain a more complete understanding of the bone microenvironment. Delineating how and why BMAT expansion occurs in various settings and whether this induction is regulated via increased sclerostin and/or decreased hPTH may provide insight into new therapies for the maintenance of healthy skeletal metabolism [3]. It is likely that the effects we observed due to bone anabolic agents were due to effects directly on the osteo/adipoprecursor, as well as subsequent indirect effects (e.g. the effect of mature osteoblasts on MSCs or on adipocytes). More research is needed to investigate if responses were due to direct or indirect effects, or both, on mature, fully-differentiated cells, MSCs, or an intermediate cell type (i.e. a pre-osteoblast or pre-adipocyte) [1]. Overall, our study adds evidence to the ties between bone and BMAT, and supports the

importance of both sclerostin and hPTH in the regulation of differentiation of these tissues. Our work also highlights the importance of investigating the bone-BMAT relationship (direct and indirect), and describes the roles of bone-derived signals (sclerostin) and hormones derived from the periphery (hPTH) in governing bone marrow adiposity in rats.

5. Conclusion

Many studies suggest that BMAT is inversely correlated with bone mineral density [43,44], and that BMAT expansion may occur during times of increased organismal stress [45] and/or damage [10], and may impact skeletal health [4,46]. Our work helps to illuminate the bone-BMAT relationship by describing the effects osteoanabolic agents have on adipocytes, which may be applicable in certain diseases or states of elevated BMAT. Histological examination of number, size, and location of adipocytes provides a cell-level examination of the bone marrow niche that in many ways gives more insight into the biology, origin and pathology of BM adipocytes than can be provided by osmium tetroxide microCT staining. Our analysis found that male and female Sprague-Dawley rats have sex-based differences in their initial trabecular bone and BMAT volumes, as well as in their response to osteoanabolic agents (Scl-Ab and hPTH), after short-term and chronic drug administration. Male rats demonstrated a significant, inverse correlation between bone and BMAT after 26-week treatments for each osteoanabolic agent. This work provides insight into the responsiveness of the bone marrow microenvironment to osteoanabolic agents. Our study also developed a novel, ImageJ-based method to quantify adipocytes and trabecular bone volume in histology slides, which can be applied to any histological bone slides of interest.

Supplementary data to this article can be found online at https://doi.org/10.1016/j.bone.2019.03.038.

Conflicts of interest

Amgen Inc. and UCB Pharma funded the original study of Ominsky et al. [1] and provided the slides to the Reagan laboratory (on loan) for re-analysis.

Funding

Support was from the NIH's National Institute of General Medical Science from: the Phase I COBRE in Metabolic Networks (P20GM121301), a pilot project from NIH P30 GM106391, Phase III COBRE in Progenitor Cells, and the U54GM115516 administrative core. The authors' work is supported by an American Cancer Society Research Grant #IRG-16-191-33, the NIH/NIDDK (R24 DK092759-01), a pilot from Harvard's Skeletal Phenotyping Core (NIH/NIAMS P30 AR066261), and start-up funds from the Maine Medical Center Research Institute.

Conflicts of Interest for this work

The other authors have no conflicts of interest.

Disclosure summary

Ominsky et al. [1] provided the histology slides for this study. Amgen Inc. and UCB Pharma funded the original study of Ominsky et al. 2015. Bone. 81: 380–391.

Acknowledgements

The histology slides used in this study were provided by Dr. Rogely Boyce from the publication Ominsky et al. 2015. The authors are thankful to Peter Cardonna, Core Manger of the Histology and Imaging Core at the University of New England for providing access to the Keyence Fluorescence Microscope BZ-X700 for image stitching. This research utilized services from core facilities and project funding at Maine Medical Center Research Institute, supported by NIH/NIGMS P20GM121301 (L. Liaw, PI), U54GM115516 (C. Rosen, PI), and P30GM106391 (R. Friesel, PI). We also thank Drs. Janaina da Silva Martins and Dr. Marie Demay at the Massachusetts General Hospital's Center for Skeletal Research Histology core for performing the OsteoMeasure analysis, funded by NIAMS P30 AR066261.

References

[1] M.S. Ominsky, D.L. Brown, G. Van, D. Cordover, E. Pacheco, E. Frazier, L. Cherepow, M. Higgins-Garn, J.I. Aguirre, T.J. Wronski, M. Stolina, L. Zhou, I. Pyrah, R.W. Boyce, Differential temporal effects of sclerostin antibody and parathyroid hormone on cancellous and cortical bone and quantitative differences in effects on the osteoblast lineage in young intact rats, Bone 81 (2015) 380–391, https://doi.org/10.1016/j.bone.2015.08.007.

[2] H. Fairfield, C. Falank, E. Harris, V. Demambro, M. McDonald, J.A.J. Pettitt, S.T. Mohanty, P. Croucher, I. Kramer, M. Kneissel, C.J. Rosen, M.R. Reagan, The skeletal cell-derived molecule sclerostin drives bone marrow adipogenesis, J. Cell. Physiol. 233 (2017) 1156–1167, https://doi.org/10.1002/jcp.25976.

[3] S.P. Kim, J.L. Frey, Z. Li, P. Kushwaha, M.L. Zoch, R.E. Tomlinson, H. Da, S. Aja, H.L. Noh, J.K. Kim, M.A. Hussain, D.L.J. Thorek, M.J. Wolfgang, R.C. Riddle, Sclerostin influences body composition by regulating catabolic and anabolic metabolism in adipocytes, Proc. Natl. Acad. Sci. U. S. A. 114 (2017) E11238–E11247, https://doi.org/10.1073/pnas.1707876115.

[4] E.L. Scheller, Rosen, What's the matter with MAT? Marrow adipose tissue, metabolism, and skeletal health, Ann. N. Y. Acad. Sci. 1311 (2014) 14–30, https://doi.org/10.1111/nyas.12327.

[5] K.J. Suchacki, W.P. Cawthorn, C.J. Rosen, Bone marrow adipose tissue: formation, function and regulation, Curr. Opin. Pharmacol. 28 (2016) 50–56, https://doi.org/10.1016/j.coph.2016.03.001.

[6] M.J. Devlin, C.J. Rosen, The bone-fat interface: basic and clinical implications of marrow adiposity, Lancet Diabetes Endocrinol. 3 (2015) 141–147, https://doi.org/10.1016/S2213-8587(14)70007-5.

[7] S. Bornstein, M. Moschetta, Y. Kawano, A. Sacco, D. Huynh, D. Brooks, S. Manier, H. Fairfield, C. Falank, A.M. Roccaro, K. Nagano, R. Baron, M. Bouxein, C. Vary, I.M. Ghobrial, C.J. Rosen, M.R. Reagan, Metformin affects cortical bone mass and marrow adiposity in diet-induced obesity in male mice, Endocrinology 158 (2017) 3369–3385, https://doi.org/10.1210/en.2017-00299.

[8] M.M. McDonald, H. Fairfield, C. Falank, M.R. Reagan, Adipose, bone, and myeloma: contributions from the microenvironment, Calcif. Tissue Int. 100 (2017) 433–448, https://doi.org/10.1007/s00223-016-0162-2.

[9] E.L. Scheller, C.R. Doucette, B.S. Learman, W.P. Cawthorn, S. Khandaker, B. Schell, B. Wu, S.-Y. Ding, M.A. Bredella, P.K. Fazeli, B. Khoury, K.J. Jepsen, P.F. Pilch, A. Klibanski, C.J. Rosen, O.A. MacDougald, Region-specific variation in the properties of skeletal adipocytes reveals regulated and constitutive marrow adipose tissues, Nat. Commun. 6 (2015) 7808, https://doi.org/10.1038/ncomms8808.

[10] B.O. Zhou, H. Yu, R. Yue, Z. Zhao, J.J. Rios, O. Naveiras, S.J. Morrison, Bone marrow adipocytes promote the regeneration of stem cells and haematopoiesis by secreting SCF, Nat. Cell Biol. 19 (2017) 891–903, https://doi.org/10.1038/ncb3570.

[11] R.T. Turner, S.A. Martin, U.T. Iwaniec, Metabolic coupling between bone marrow adipose tissue and hematopoiesis, Curr. Osteoporos. Rep. 16 (2018) 95–104, https://doi.org/10.1007/s11914-018-0422-3.

[12] M.S. Ominsky, R.W. Boyce, X. Li, H.Z. Ke, Effects of sclerostin antibodies in animal models of osteoporosis, Bone 96 (2017) 63–75, https://doi.org/10.1016/j.bone.2016.10.019.

[13] H. Fairfield, C.J. Rosen, M.R. Reagan, Connecting bone and fat: the potential role for Sclerostin, Curr. Mol. Biol. Reports. 3 (2017) 114–121, https://doi.org/10.1007/s40610-017-0057-7.

[14] G.J. Spencer, Wnt signalling in osteoblasts regulates expression of the receptor activator of NF B ligand and inhibits osteoclastogenesis in vitro, J. Cell Sci. 119 (2006) 1283–1296, https://doi.org/10.1242/jcs.02883.

[15] D.A. Glass, P. Bialek, J.D. Ahn, M. Starbuck, M.S. Patel, H. Clevers, M.M. Taketo, F. Long, A.P. McMahon, R.A. Lang, G. Karsenty, Canonical Wnt signaling in differentiated osteoblasts controls osteoclast differentiation, Dev. Cell 8 (2005) 751–764, https://doi.org/10.1016/j.devcel.2005.02.017.

[16] S. Taylor, M.S. Ominsky, R. Hu, E. Pacheco, Y.D. He, D.L. Brown, J.I. Aguirre, T.J. Wronski, S. Buntich, C.A. Afshari, I. Pyrah, P. Nioi, R.W. Boyce, Time-dependent cellular and transcriptional changes in the osteoblast lineage associated with sclerostin antibody treatment in ovariectomized rats, Bone 84 (2016) 148–159, https://doi.org/10.1016/j.bone.2015.12.013.

[17] M.M. McDonald, M.R. Reagan, S.E. Youlten, S.T. Mohanty, A. Seckinger, R.L. Terry, J.A. Pettitt, M.K. Simic, T.L. Cheng, A. Morse, L.M.T. Le, D. Abi-Hanna, I. Kramer, C. Falank, H. Fairfield, I.M. Ghobrial, P.A. Baldock, D.G. Little, M. Kneissel, K. Vanderkerken, J.H.D. Bassett, G.R. Williams, B.O. Oyajobi, D. Hose, T.G. Phan, P.I. Croucher, Inhibiting the osteocyte-specific protein sclerostin increases bone mass and fracture resistance in multiple myeloma, Blood 129 (2017) 3452–3464, https://doi.org/10.1182/blood-2017-03-773341.

[18] D.H. Balani, H.M. Kronenberg, Withdrawal of parathyroid hormone after prolonged

administration leads to adipogenic differentiation of mesenchymal precursors in vivo, Bone (2018), https://doi.org/10.1016/j.bone.2018.05.024.
[19] J. Wu, X.-H. Cai, X.-X. Qin, Y.-X. Liu, The effects of sclerostin antibody plus parathyroid hormone (1–34) on bone formation in ovariectomized rats, Z. Gerontol. Geriatr. (2017), https://doi.org/10.1007/s00391-017-1219-1.
[20] N.H. Kulkarni, D.L. Halladay, R.R. Miles, L.M. Gilbert, C.A. Frolik, R.J.S. Galvin, T.J. Martin, M.T. Gillespie, J.E. Onyia, Effects of parathyroid hormone on Wnt signaling pathway in bone, J. Cell. Biochem. 95 (2005) 1178–1190, https://doi.org/10.1002/jcb.20506.
[21] N.A. Sims, C. Vrahnas, Regulation of cortical and trabecular bone mass by communication between osteoblasts, osteocytes and osteoclasts, Arch. Biochem. Biophys. 561C (2014) 22–28, https://doi.org/10.1016/j.abb.2014.05.015.
[22] R.T. Turner, U.T. Iwaniec, Low dose parathyroid hormone maintains normal bone formation in adult male rats during rapid weight loss, Bone 48 (2011) 726–732, https://doi.org/10.1016/j.bone.2010.12.034.
[23] Y. Fan, J. Hanai, P.T. Le, R. Bi, D. Maridas, V. DeMambro, C.A. Figueroa, S. Kir, X. Zhou, M. Mannstadt, R. Baron, R.T. Bronson, M.C. Horowitz, J.Y. Wu, J.P. Bilezikian, D.W. Dempster, C.J. Rosen, B. Lanske, Parathyroid hormone directs bone marrow mesenchymal cell fate, Cell Metab. 25 (2017) 661–672, https://doi.org/10.1016/j.cmet.2017.01.001.
[24] D.H. Balani, N. Ono, H.M. Kronenberg, Parathyroid hormone regulates fates of murine osteoblast precursors in vivo, J. Clin. Invest. (2017), https://doi.org/10.1172/JCI91699.
[25] D.W. Dempster, J.E. Compston, M.K. Drezner, F.H. Glorieux, J.A. Kanis, H. Malluche, P.J. Meunier, S.M. Ott, R.R. Recker, A.M. Parfitt, Standardized nomenclature, symbols, and units for bone histomorphometry: a 2012 update of the report of the ASBMR Histomorphometry nomenclature committee, J. Bone Miner. Res. 28 (2013) 2–17, https://doi.org/10.1002/jbmr.1805.
[26] C.A. Schneider, W.S. Rasband, K.W. Eliceiri, NIH image to ImageJ: 25 years of image analysis, Nat. Methods 97 (2012) (2012).
[27] W.R.T. Ferreira, ImageJ User Guide IJ 1.46r, IJ 1.46r, vol. 185, (2012), https://doi.org/10.1038/nmeth.2019.
[28] K. Eliceiri, C.A. Schneider, W.S. Rasband, K.W. Eliceiri, NIH image to ImageJ: 25 years of image analysis HISTORICAL commentary NIH image to ImageJ: 25 years of image analysis, Nat. Methods 9 (2012) 671–675, https://doi.org/10.1038/nmeth.2089.
[29] P. Sengupta, The laboratory rat: relating its age with human's, Int. J. Prev. Med. 4 (2013) 624–630 (doi:23930179).
[30] M.S. Wolfe, L. Klein, Sex differences in absolute rates of bone resorption in young rats: appendicular versus axial bones, Calcif. Tissue Int. 59 (1996) 51–57.
[31] D. Yilmaz, B. Ersoy, E. Bilgin, G. Gümüşer, E. Onur, E.D. Pinar, Bone mineral density in girls and boys at different pubertal stages: relation with gonadal steroids, bone formation markers, and growth parameters, J. Bone Miner. Metab. 23 (2005) 476–482, https://doi.org/10.1007/s00774-005-0631-6.
[32] S. Stagi, L. Cavalli, S. Ricci, M. Mola, C. Marchi, S. Seminara, M.L. Brandi, M. de Martino, Parathyroid hormone levels in healthy children and adolescents, Horm. Res. Paediatr. 84 (2015) 124–129, https://doi.org/10.1159/000432399.
[33] S. Minisola, M.T. Pacitti, A. Scarda, R. Rosso, E. Romagnoli, V. Carnevale, L. Scarnecchia, G.F. Mazzuoli, Serum ionized calcium, parathyroid hormone and related variables: effect of age and sex, Bone Miner 23 (1993) 183–193.
[34] A.R. Altman, W.J. Tseng, C.M.J. de Bakker, A. Chandra, S. Lan, B.K. Huh, S. Luo, M.B. Leonard, L. Qin, X.S. Liu, Quantification of skeletal growth, modeling, and remodeling by in vivo micro computed tomography, Bone 81 (2015) 370–379, https://doi.org/10.1016/j.bone.2015.07.037.
[35] K.M. Beekman, A.G. Veldhuis-Vlug, M. den Heijer, M. Maas, A.M. Oleksik, M.W. Tanck, S.M. Ott, R.J. van 't Hof, P. Lips, P.H. Bisschop, N. Bravenboer, The effect of raloxifene on bone marrow adipose tissue and bone turnover in postmenopausal women with osteoporosis, Bone 118 (2019) 62–68, https://doi.org/10.1016/j.bone.2017.10.011.
[36] P.D. Delmas, N.H. Bjarnason, B.H. Mitlak, A.-C. Ravoux, A.S. Shah, W.J. Huster, M. Draper, C. Christiansen, Effects of raloxifene on bone mineral density, serum cholesterol concentrations, and uterine endometrium in postmenopausal women, N. Engl. J. Med. 337 (1997) 1641–1647, https://doi.org/10.1056/NEJM199712043372301.
[37] S.M. Ott, A. Oleksik, Y. Lu, K. Harper, P. Lips, Bone histomorphometric and biochemical marker results of a 2-year placebo-controlled trial of raloxifene in postmenopausal women, J. Bone Miner. Res. 17 (2002) 341–348, https://doi.org/10.1359/jbmr.2002.17.2.341.
[38] G. Duque, W. Li, M. Adams, S. Xu, R. Phipps, Effects of risedronate on bone marrow adipocytes in postmenopausal women, Osteoporos. Int. 22 (2011) 1547–1553, https://doi.org/10.1007/s00198-010-1353-8.
[39] J. Jin, L. Wang, X.K. Wang, P.L. Lai, M.J. Huang, D. Di Jin, Z.M. Zhong, J.T. Chen, X.C. Bai, Risedronate inhibits bone marrow mesenchymal stem cell adipogenesis and switches RANKL/OPG ratio to impair osteoclast differentiation, J. Surg. Res. 180 (2013) e21–e29, https://doi.org/10.1016/j.jss.2012.03.018.
[40] A. Casado-Díaz, R. Santiago-Mora, G. Dorado, J.M. Quesada-Gómez, Risedronate positively affects osteogenic differentiation of human mesenchymal stromal cells, Arch. Med. Res. 44 (2013) 325–334, https://doi.org/10.1016/j.arcmed.2013.05.002.
[41] N.H. Kulkarni, T. Wei, A. Kumar, E.R. Dow, T.R. Stewart, J. Shou, M. N'cho, D.L. Sterchi, B.D. Gitter, R.E. Higgs, D.L. Halladay, T.A. Engler, T.J. Martin, H.U. Bryant, Y.L. Ma, J.E. Onyia, Changes in osteoblast, chondrocyte, and adipocyte lineages mediate the bone anabolic actions of PTH and small molecule GSK-3 inhibitor, J. Cell. Biochem. 102 (2007) 1504–1518, https://doi.org/10.1002/jcb.21374.
[42] D.J. Rickard, F.-L. Wang, A.-M. Rodriguez-Rojas, Z. Wu, W.J. Trice, S.J. Hoffman, B. Votta, G.B. Stroup, S. Kumar, M.E. Nuttall, Intermittent treatment with parathyroid hormone (PTH) as well as a non-peptide small molecule agonist of the PTH1 receptor inhibits adipocyte differentiation in human bone marrow stromal cells, Bone 39 (2006) 1361–1372, https://doi.org/10.1016/j.bone.2006.06.010.
[43] W. Shen, J. Chen, M. Punyanitya, S. Shapses, S. Heshka, S.B. Heymsfield, MRI-measured bone marrow adipose tissue is inversely related to DXA-measured bone mineral in Caucasian women, Osteoporos. Int. 18 (2007) 641–647, https://doi.org/10.1007/s00198-006-0285-9.
[44] W. Shen, R. Scherzer, M. Gantz, J. Chen, M. Punyanitya, C.E. Lewis, C. Grunfeld, Relationship between MRI-measured bone marrow adipose tissue and hip and spine bone mineral density in African-American and Caucasian participants: the CARDIA study, J. Clin. Endocrinol. Metab. 97 (2012) 1337–1346, https://doi.org/10.1210/jc.2011-2605.
[45] M.J. Devlin, Why does starvation make bones fat? Am. J. Hum. Biol. 23 (2011) 577–585, https://doi.org/10.1002/ajhb.21202.
[46] Z. Li, J. Hardij, D.P. Bagchi, E.L. Scheller, O.A. MacDougald, Development, regulation, metabolism and function of bone marrow adipose tissues, Bone 110 (2018) 134–140, https://doi.org/10.1016/j.bone.2018.01.008.